Vol. 46, No. 4 (2024) 651-663, DOI: 10.24874/ti.1654.03.24.10

Tribology in Industry

www.tribology.rs

RESEARCH

Wear Performance of Wire Arc AM SS 316L Plate For Different Thermal History Regions

Abdulrahman Alrumayh[a,*]

[a]*Department of Mechanical Engineering, College of Engineering, Qassim University, Buraydah, 51431, Saudi Arabia*

Keywords:

Sliding wear
Steel
Hardness
WAAM
AM

* Corresponding author:

Abdulrahman Alrumayh
E-mail: A.Alrumayh@qu.edu.sa

Received: 30 March 2024
Revised: 2 April 2024
Accepted: 28 October 2024

A B S T R A C T

The development of metal Additive Manufacturing AM processes has become promising for different applications and sectors, especially 316L austenitic stainless steel. Compared with polymer AM which has reached near maturity in process parameters and product properties, metal AM processes have enormous areas for research. Wire Arc AM (WAAM) has a high deposition rate and high heat input, which changes material properties in many ways. For example, wear rate has been studied in AM and WAAM, especially for different materials and parameters. This study aims to investigate the difference between the wear behaviors for different regions in WAAM printed samples. The regions have different thermal cycle histories and different hardness levels. A sample was printed by WAAM and prepared for wear test measurement. There are two selected areas, the inter-layer IL, and the middle of the layer IM which have different thermal cycles. The coefficient of friction COF, COF slope, Friction force, volume loss and mass loss, and hardness were measured and calculated for these two areas. The results show that the IL areas have lower COF, negative COF slope, and lower hardness than other areas. That can be the result of the thermal cycle which affects the residual stress.

1. INTRODUCTION

Additive Manufacturing (AM) processes have shown potential for complex and customized products. There are different approaches to categorizing these processes: according to material, heat source, etc. Metal AM has also been classified according to these approaches. Metals can be additively manufactured (AM-ed) by different processes, such as selective laser melting (SLM) [1] or selective laser sintering (SLS) [2], cold spraying AM (CSAM) [3], or wire metal AM (WAAM) [4,5]. In metal AM there are drawbacks for several processes. One of them is distortion and a high level of residual stress. It appears in high heat input processes such as direct energy deposition DED especially (WAAM) [6]. When using this technology, the level of these drawbacks can differ from one material to another [7]. One of the main metals used in WAAM is stainless steel 316L, for its preferred properties [7,8]. Also, 316 has been used in different printing processes [9].

One standardized wear test is the ball-on-flat test [10], Regarding the friction wear performance of materials, including the AM-ed ones, the ball-on-flat test is a standard test widely used to evaluate their performance under friction conditions. There are some studies investigating how the deposition of coatings enhances the wear rate for different materials, for instance, the wear rate has a reduction of 50% by using various cermet coatings on CF-PEEK sliding against 17-4PH [11], as an example for the base material and different conditions, with low alloy steel the sliding wear shows enhancing I the level with 400°C but decreasing with 600°C [12], for Ti-6Al-4V large pulse electron beam (LPEB) irradiation and plasma electrolytic oxidation (PEO) were introduced and improved the wear behavior [13]. For different materials such as Al7075, the wear rate is higher at elevated temperatures [14]. SLS Polyamide-12 with using such as graphite and molybdenum disulfide as solid lubricants has a direct improvement on the wear rate [15] Also for different materials such as Inconel 718, it was emphasized that optimizing additive manufacturing parameters will lead to improving wear performance of In718 [16]. Also, In718 was studied at different temperatures, and it showed that the friction coefficient increased with higher temperatures [17]. Using SLM with Inconel 625 and different test temperatures has shown a higher wear rate as well [18]. Another method for fabrication of In625 with laser cladding coating proves that using In625 and tungsten carbide will lower the wear rate [19]. Also for different materials such as steel H13, the building strategies in AM will lead to changes in the wear rate [20]. Process parameters to enhance the behavior of cemented carbide have been studied [21]. When comparing wrought 316 with arc-melting elemental Ni-Co-Cr, 316 has shown a higher value of wear rate [22]. Others used different materials to test their contact with each other in terms of wear behavior [23]. The behavior of different types of steel against steel and ceramics at high temperatures has been studied as well [24], polyetheretherketone against AISI 630 [25].

The importance of wear behavior testing is embedded in the applications, as it has been beneficial for studying the implants' wear in different environments [26] and also for different corrosion applications such as tribo-corrosion [27], and corrosion under marine environments [28]. Also, advanced ceramics for potential space applications have been tested [29]. Another process of AM, binder jetting printing has shown different levels of COF for 316 stainless steel "SS" [30]. SS 316 has also gained research history for its wear behavior. In a comparison of different processing methods, casting has around 0.55 COF, while SLM has 0.5 COF, hot pressing has 0.53 COF, and CSAM has 0.85 COF [31,32]. Building direction and laser power affect SLM 316 products [33]. The temperature of the test also affects the wear rate [34] and shows that the wear rate in SLM 316 has a lower level than wrought 316 in a 300-400 °C environment [35]. The surfaces of the SLM printed sample of 316 showed COF levels between 0.3 to 0.45 at the end of the test [36].

Treatments have also affected the wear behavior of 316. The cyaniding process has improved the wear resistance [37]. Adding boron to 316 reduced the COF by about 3% [38].

It has been reported that there is a difference between the wear rate for samples taken at the beginning, middle, and end of a WAAM printed plate, the difference can be more than 100% of the wear rate [39]. 316L has been used in composite material combined with SiCp and AM-ed by the DED process. Using SiCp has shown an increase in the COF, but a reduction in the wear rate for different percentages of SiCp [40]. Using SLM did not show a difference in the wear rate if the test was done in different directions of the faces, but the scratch test has shown some differences [41]. Building direction did not show any remarkable change in COF or wear direction for 316L printed by SLM [42]. Using high-pressure torsion for 316L plates printed by SLM has shown improvement in the wear rate [43]. Introducing heat treatment to the 316L sample, which was AM-ed by using direct laser metal sintering, has shown an increase in the wear rate [44]. So this research investigates the change in the wear behavior and hardness level of different areas in a plate printed by WAAM for SS 316L. The interesting areas are the between layers and the layers themselves since there are different thermal cycles, which may lead to different mechanical behavior.

2. MATERIAL AND METHODS

Literature on the WAAM manufacturing process shows great potential in Big Area AM, which deposits large amounts of material compared to other AM processes. At Qassim University, the WAAM process used a Borunte 6-axis robot with an Ehave CM350 welding machine.

There are some interesting areas for testing, which is explained as in WAAM, the layers have two areas, the area of deposited material and the re-melted area. These areas are different. Fig. 1 shows a cross-section from a WAAM-printed plate cut by a saw, polished, and electrically etched. Fig. 1 shows the area of the deposited layers between the black curves, and the re-melted areas are circled in white. These re-melted areas have a different thermal and mechanical history than the rest of the deposited layers. Also, the area between the layers has different residual stress for specific heat inputs as shown in Fig. 1 [1].

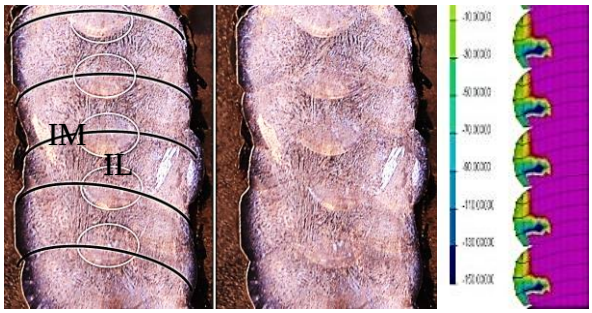

Fig. 1. Cross-section of WAAM printed components [1].

Since these areas are different, this research aims to investigate the wear behavior of these two areas. The sample is a piece of a plate that was printed using SS 316L 0.8 mm wire. The plate is 14 layers and 150 mm in length, with 20 V, and 140 A for current, and 3 mm/s for speed. Fig. 2 is a 316L printed plate with two areas, area A which will be sawed into a rectangular sample, and then cut in half to get the middle area as described in Fig. 3, and area B, which is a cross-section piece of the plate.

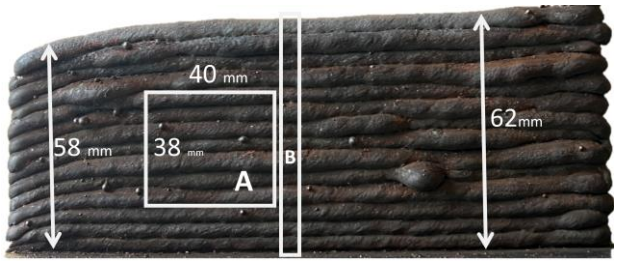

Fig. 2. The printed plate, with area A) for wear performance sample B) the cross-section sample.

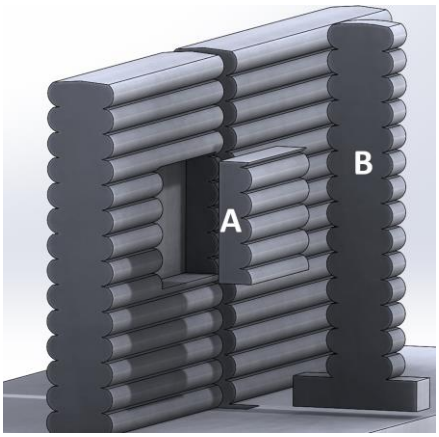

Fig. 3. The two-piece sample from the plate.

Pieces, A & B, are shown in Fig. 4, (A) piece is the wear sample, and (B) piece is a cross-section sample that is associated with the wear sample. The wear sample is an 8-layer sample that was cut, polished, and electrically etched. The aim is to get the re-melted interlayer area again, as described in Fig. 1, and it appears in Fig. 4. This research is to measure the wear performance of the two areas IM (in the Middle of Layers) and IL (InterLayer) with different parameters including force (20, 40, 60 N), speed (3, 6 mm/s), no lubrication (dry), oil, and lubrication (Wet) condition and the ball has a diameter of 10 mm and it is made out of hardened steel. The parameters of the wear cases are described in Table 1. The wear test used Bruker UMT TriboLab Fig. 5 for measuring the COF and the friction force. Measuring the micro-hardness of these two areas by using Qualitest's Digital Micro Vickers Hardness Tester - QV-1000 in IL and IM areas; the hardness Force is 9.808 N, and the indenter angle is 136°. The results of the wear tests have noise, so for visualization purposes in the figure, the data will be smoothed using the least squares method. The original data will be fitted to a linear equation to get the shift value b and the slope *m, f(x) = mx + b.*

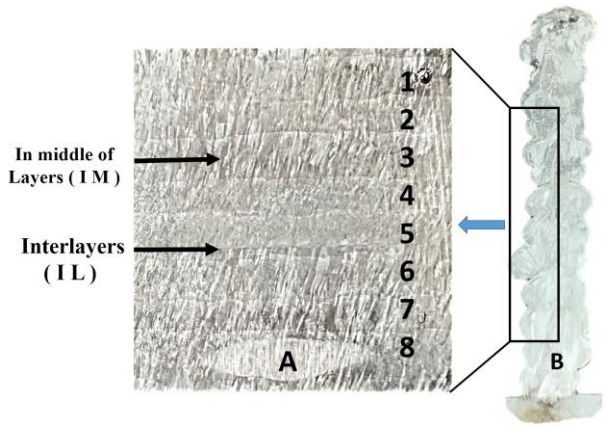

Fig. 4. A & B pieces of the printed plate.

Table 1. Wear performance cases.

Case	Name and place	Dry/Wet	Fz (N)	Speed
1	IM	Dry	20	3
2	IM	Dry	40	3
3	IM	Dry	60	3
7	IM	Dry	20	6
8	IM	Dry	40	6
9	IM	Dry	60	6
10	IM	Wet	20	6
11	IM	Wet	40	6
12	IM	Wet	60	6
13	IL	Dry	20	3
14	IL	Dry	40	3
15	IL	Dry	60	3
16	IL	Wet	20	3
17	IL	Wet	40	3
18	IL	Wet	60	3
19	IL	Wet	20	6
20	IL	Wet	40	6
21	IL	Wet	60	6

Fig. 5. Bruker UMT TriboLab.

The volume loss of these cases was calculated by using the maximum depth of the ball in the sample h to get the segment of the circle of the spherical cap of the ball as in equ.1; the shaded area in Fig. 6, then multiply the area by the length of the stroke L, which is 10 mm.

$$A = R^2\, cos^{-1}\left(\frac{R-h}{R}\right) - (R-h) * \sqrt{R^2 - (R^2 - h^2)} \quad (1)$$

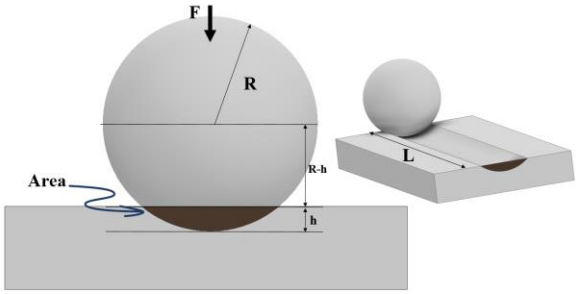

Fig. 6. Ball on flat as describing the volume loss.

The wear rate was calculated by using equ.2, where V is the volume loss, L is the stroke length, and F is the normal force applied to the sample [45].

$$WearRate = \frac{V}{L\,F} \quad (2)$$

3. RESULTS AND DISCUSSION

3.1 COF

Fig. 7. COF for dry IM and IL with different forces and fixed speed shows smoothed data with the fitted curves for COF curves that were measured for IM and IL areas from a 316L AM-ed plate. The parameters are fixed speed, 3 mm/s, for dry cases with different forces. It seems that the trend is the same for both cases, the COF is around 0.6 except for force 20 for the IL area, which has the lower rate. Even for the other forces IL cases have a lower rate of about 0.02 difference. Fig. 8. COF for Wet IM and IL with different forces and fixed speed shows speed (6 mm/s) cases with Wet surface, and the highest COF values (around 0.1) are IM cases with low and high force 20-60N. While the lower COF values are in IL cases with 20N as in dry cases. Also, an IM dry case with 40N has a lower rate than a 40N IL case.

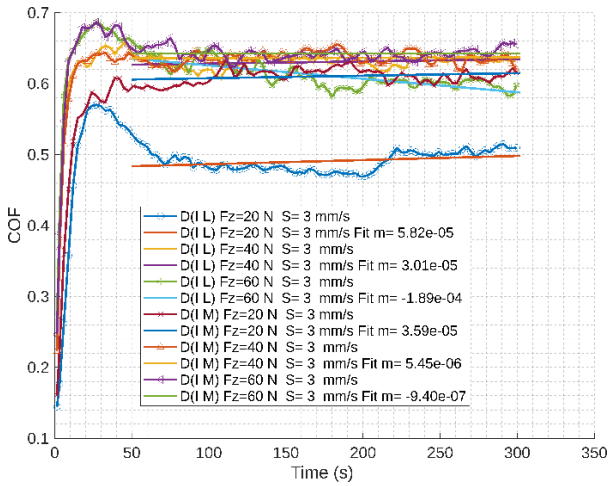

Fig. 7. COF for dry IM and IL with different forces and fixed speed.

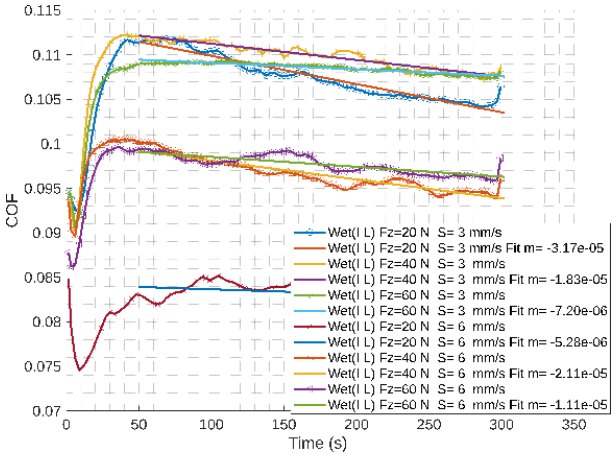

Fig. 8. COF for Wet IM and IL with different forces and fixed speed.

Fig. 9. COF for dry and Wet IM with different forces and fixed speed shows the COF values for dry and Wet IM cases. As shown, the COF of the AM-ed 316L plate is around 0.54 for the dry case and around 0.1 for the Wet case. The COF for the dry case is 5 times that of the Wet case for the speed of 6 mm/s. The applied force does not seem to make much of a difference in the value of the COF but plays a role in the slope of this friction, which is described in another section. Fig. 10. COF for dry and Wet IL with different forces shows the COF for IL for both cases, dry and Wet, with a speed of 3 mm/s, as shown for the Wet cases IL has 0.11 which is higher than the area IM. In addition, IL dry cases also have a higher value of about 0.63 for forces 40 and 60 N which is also higher than the IM cases with speeds of 6 mm/s. While for 20N the COF is around 0.5 which is lower than the IM case. Here speed affects these results, but the obvious effect is that of the lubrication on the value of COF.

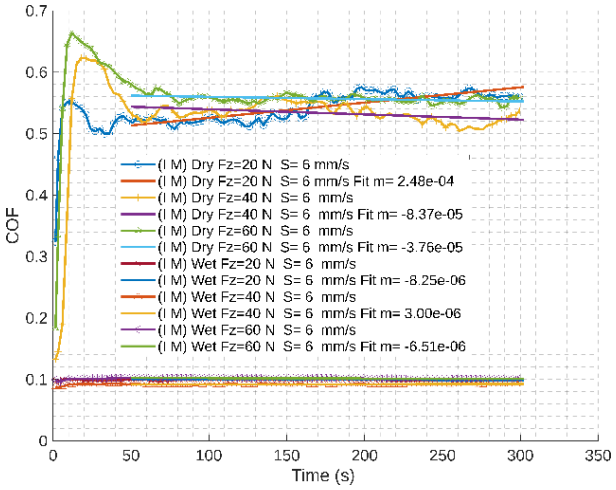

Fig. 9. COF for dry and Wet IM with different forces and fixed speed.

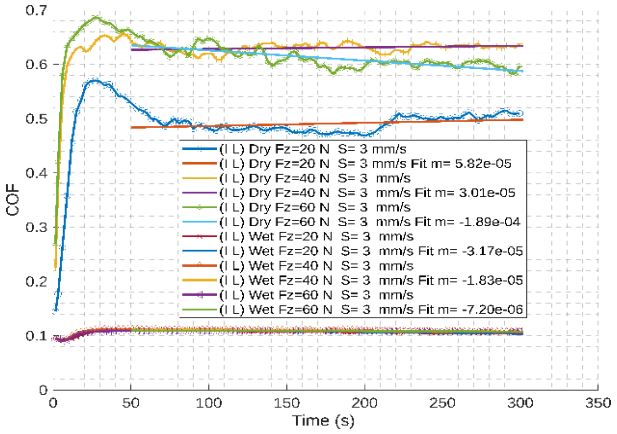

Fig. 10. COF for dry and Wet IL with different forces.

To show the effect of speed on COF, Fig. 12. COF for Wet IL with different forces and different speeds, and Fig. 11. COF for dry IM with different forces and speeds, show the IM dry cases and IL Wet cases with the same different forces as well as different speeds. In Fig. 11, the speed change from 3 to 6 mm/s has lowered the level of COF for IM cases in the dry condition. The range of COF can reach around 0.1 between the cases. In Fig. 12, for IL cases with the Wet condition, the speed has also lowered the COF, with a range of 0.01 of COF.

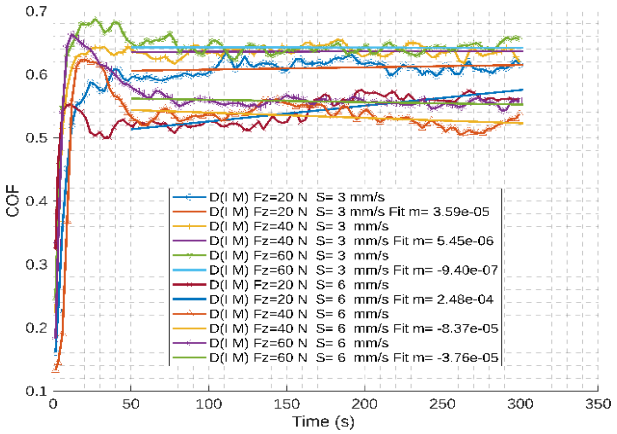

Fig. 11. COF for dry IM with different forces and speed.

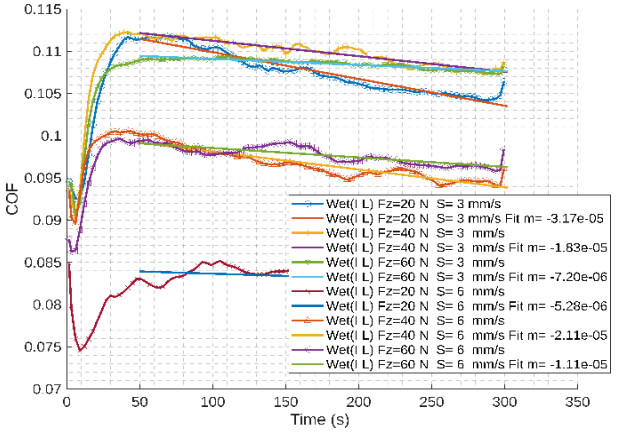

Fig. 12. COF for Wet IL with different forces and different speed.

COF has different mean values for each case, also the trend of the value is very important. Therefore, the mean value was calculated by the arithmetic mean method. Fig. 13 and Table 2 show the mean values of COF.

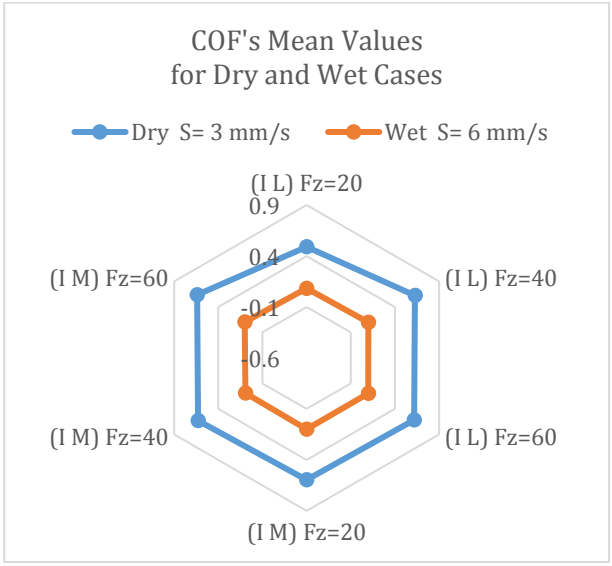

(a)

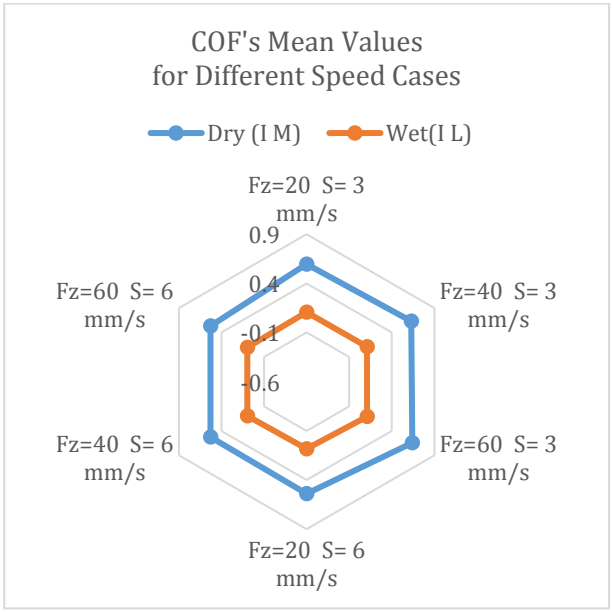

(b)

Fig. 13. Polar chart for the mean value of COF, up (a) two speeds comparison, down (b) dry and Wet tests comparison.

Fig. 13 A shows the difference between the mean for two different speeds, Dry 3- Wet 6 mm/s. In the dry case with a speed of 3 mm/s, IL shows a lower average than IM cases, also, the range in IL is larger by more than 50% as appeared in Table 2. The same observation appeared in the Wet case with higher speed. IL has a lower average but a larger range than IM cases.

Fig. 13 B shows the difference between the dry IM and Wet IL to show the effect of speed on the COF. In the dry case for IM, the speed decreased the COF average by 20% and reduced the range as well. In the Wet cases for IL, the speed effect decreased the average by 10% but increased the range.

In general, the IL cases have lower mean COF values than the IM cases. Doubling the speed increased the COF mean value by 10-20%.

Table 2. COF's mean values.

Forces and cases	Dry S= 3 mm/s	Wet S= 6 mm/s
(I L) Fz = 20 N	0.4892	0.0826
(I L) Fz = 40 N	0.6259	0.0967
(I L) Fz = 60 N	0.6152	0.0974
Average	0.57677	0.0923
Standard deviation	0.07602	0.0083
(I M) Fz = 20 N	0.5958	0.0995
(I M) Fz = 40 N	0.6294	0.092
(I M) Fz = 60 N	0.6405	0.1015
Average	0.6219	0.09767
Standard deviation	0.0232	0.00500
Forces and speed	Dry (I M)	Wet(I L)
Fz=20 N S= 3 mm/s	0.5958	0.1069
Fz=40 N S= 3 mm/s	0.6294	0.1092
Fz=60 N S= 3 mm/s	0.6405	0.1077
average	0.6219	0.107933
Standard deviation	0.02327	0.00116
Fz=20 N S= 6 mm/s	0.5395	0.0826
Fz=40 N S= 6 mm/s	0.5297	0.0967
Fz=60 N S= 6 mm/s	0.5297	0.0974
average	0.53297	0.09223
Standard deviation	0.0056580	0.00835

The trend of COF was presented as the slope of the stable value. For example, Fig. 12 shows the COF but there is the first region where the COF is not stable, which is the area at the surface, after which the COF shows a stable behavior. It is also important to mention again that the COF values vs. time in the previous curves are smoothed. So, to get a stable trend for COF over time, the first value must be excluded. So the slope was calculated by using the least squares method to fit these data into a straight line equation, with m as the gradient. Therefore, if the gradient (m) is positive it means the COF is increasing over time, while if m is negative, it means the COF is decreasing over time. Fig. 14

A shows IL and IM cases for different speeds and forces. For the dry case with 3 mm/s speed, IL has a negative average of the COF slope which means the COF will decrease; in contrast, IM has a positive average which tends to increase the COF over time. Using lubrication, as expected, has lowered the slope average, which makes the COF lower faster than the dry cases through time. In IM cases, using lubrication has changed the slope average value into a negative, which means that using lubrication reduced the COF instead of increasing it in dry cases.

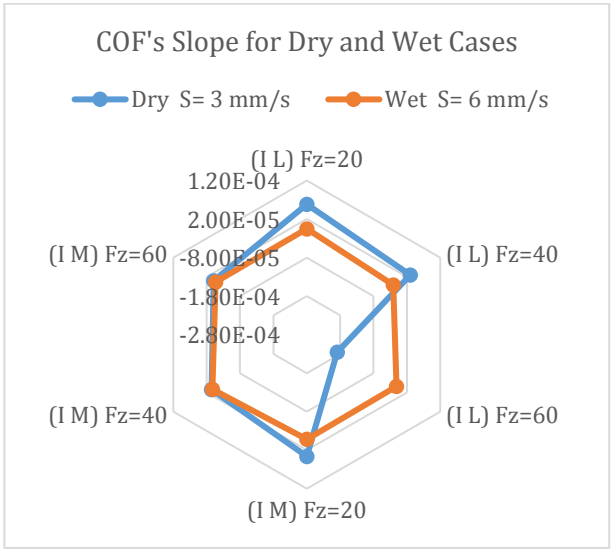

(a)

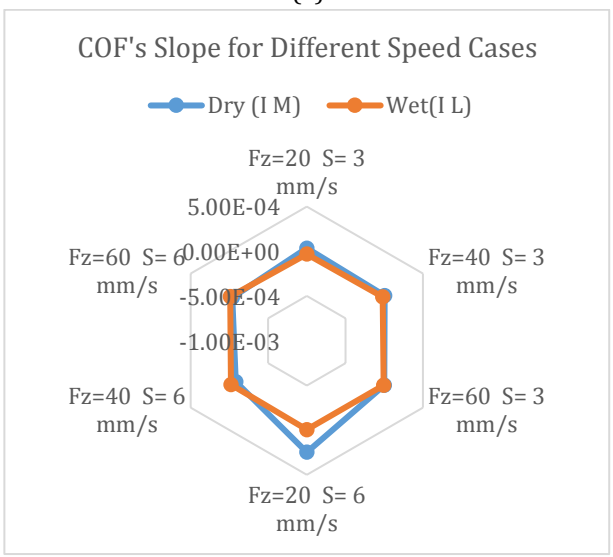

(b)

Fig. 14. Polar chart of COF slope value, up (a) two speeds comparison, down (b) dry and Wet tests comparison.

Fig. 14 B shows the effect of speed on the slope of dry and Wet cases. In dry IM cases, the speed increased the COF slope which led to an increase in the COF value over time. In Wet IL cases, in the presence of a lubricant, the speed increased the value of the average slope but it remained a negative value which means that the COF value will be reduced less over time.

In general, COF will increase for IM and will decrease for IL in dry cases, both will decrease in Wet cases and IL will decrease 3 times faster than IM. Doubling the speed will make dry IM COF increase by 3 times, but in Wet IL cases, the COF is reduced by 30%.

Table 3. COF's slope.

Forces and speed	Dry (I M)	Wet(I L)
Fz=20 S= 3 mm/s	3.59E-05	-3.17E-05
Fz=40 S= 3 mm/s	5.45E-06	-1.83E-05
Fz=60 S= 3 mm/s	-9.40E-07	-7.20E-06
Average	1.35E-05	-1.91E-05
Fz=20 S= 6 mm/s	2.48E-04	-5.28E-06
Fz=40 S= 6 mm/s	-8.37E-05	-2.11E-05
Fz=60 S= 6 mm/s	-3.76E-05	-1.11E-05
Average	4.297E-05	-1.3E-05
Forces and speed	Dry (I M)	Wet(I L)
Fz=20 S= 3 mm/s	3.59E-05	-3.17E-05
Fz=40 S= 3 mm/s	5.45E-06	-1.83E-05
Fz=60 S= 3 mm/s	-9.40E-07	-7.20E-06
Average	1.35E-05	-1.91E-05
Fz=20 S= 6 mm/s	2.48E-04	-5.28E-06
Fz=40 S= 6 mm/s	-8.37E-05	-2.11E-05
Fz=60 S= 6 mm/s	-3.76E-05	-1.11E-05
Average	4.297E-05	-1.3E-05

3.2 Volume loss and mass loss

To get the mass loss, the volume loss was multiplied by the density of 316L which is 0.008 g/mm^3. Fig. 15 shows the mass loss. From the curves, the Wet cases have higher mass loss than the dry cases by 10%, which may be caused by the wear of the ball itself. In the dry cases, this is larger, which makes the contact area larger but the depth smaller. The increase in speed has also lowered the mass loss for the larger forces, for both IL and IM cases. For Wet cases, IL has a slightly increasing mass loss than IM by around 1%. However, the dry cases show the same results only with low force, and the contrast for higher forces and 60N have the same mass loss. Fig. 16 shows the volume loss which has the same trend as the mass loss.

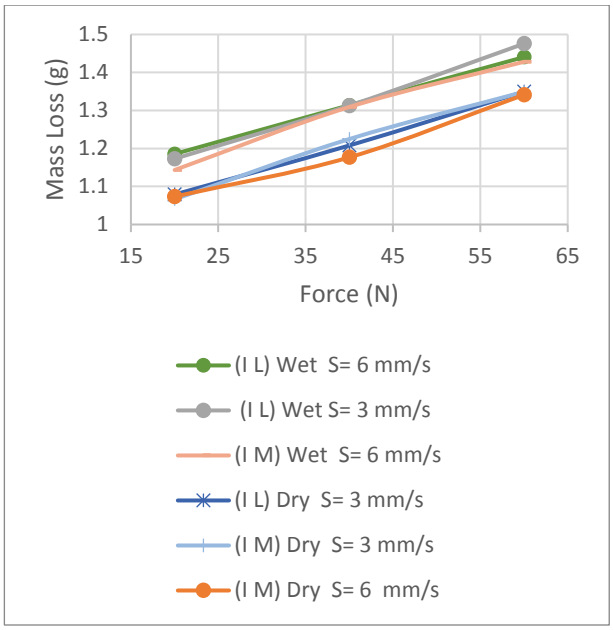

Fig. 15. Mass loss of the wear test.

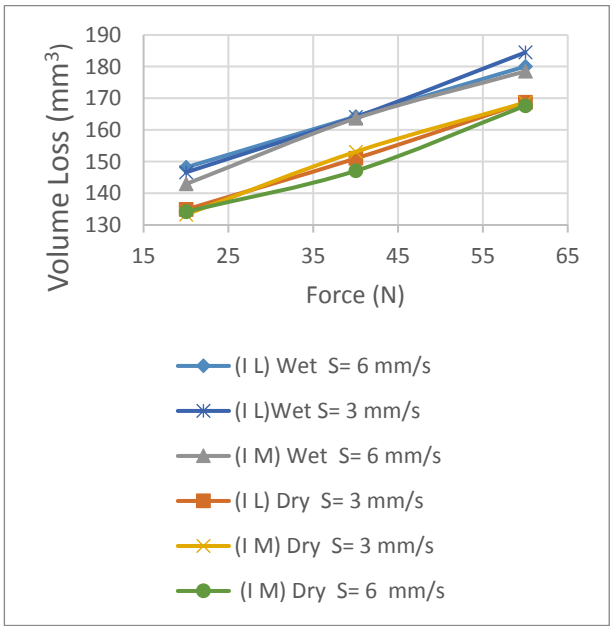

Fig. 16. Volume loss of the wear test.

3.3 Wear rate

For the wear rate Fig. 17, the environment has an effect on the wear rate for the AMed 316L plate. Lubrication increased the wear rate by 10%. Speed does not show a significant difference. Doubling the force from 20 to 40 reduced the wear rate by 25% while increasing it to 60 reduced it by 20% from the 40 N level. The main goal is to investigate the difference between IL and IM locations. For dry cases, with a speed of 3 mm/s, there is generally no significant difference, at force 20 N, the difference is near 1.5%, and IL has a larger wear rate. For Wet cases with a speed of 6mm/s, there is an average reduction of 1.5%, and the IM has a lower rate. In addition, at force 20 N, the difference is 3.5%, and IL has the larger wear rate.

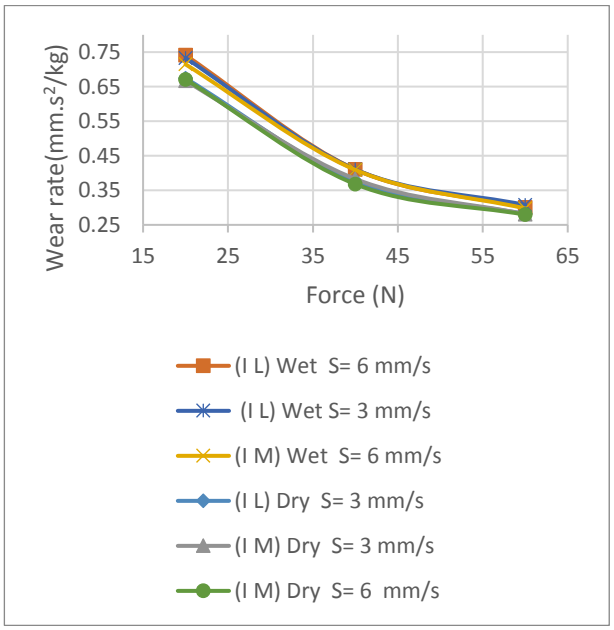

Fig. 17. Wear rate of 316L WAAM plate.

3.4 Friction force

Fig. 18 shows the friction force calculated by the square root of the squared values of other forces. The values indicate that IL cases have lower values than IM values after they stabilize. But the difference is almost 1 - 2 Newton. For the speed effect, the increase in the friction force is linearly correlated with the increase in the z force.

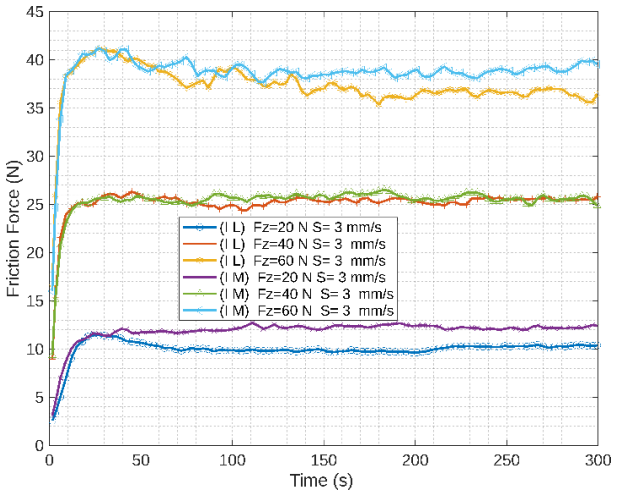

Fig. 18. Friction force for Wet IM and IL with different forces fixed speed.

Fig. 19 shows the speed of lowering the friction force by 0.1 - 0.2 Newton for IL Wet cases, also the level of the friction force is reduced over time. Especially at lower speeds. As the z force increases, the gap between the friction forces for different speeds will also increase, in the case of 20N the gap is smaller than the gap in the case of 60N.

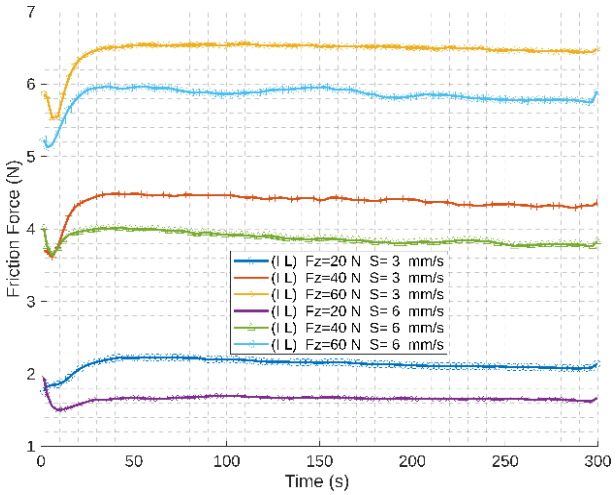

Fig. 19. Friction force for Wet IL with different forces and different speeds.

Fig. 20, even for Wet cases, IL samples show lower friction force values than the IM cases in both 20 and 60 z forces, but in 40N z force, the IL starts higher than IM, but over time it seems that IL friction force decreases and IM stabilizes, which eventually allows IM to be higher in friction force value.

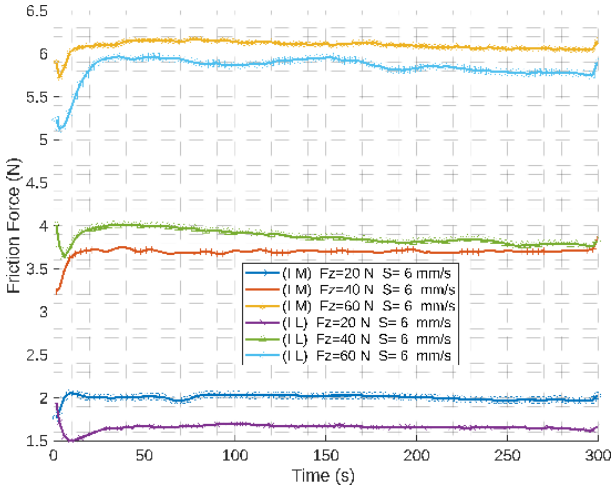

Fig. 20. Friction force for Wet IM and IL with different forces fixed speed.

Fig. 21 In IM dry cases, the speed has shown a clear effect of the value of friction force, with the same notes on IL cases, the increase in z force will increase the gap between the speed cases.

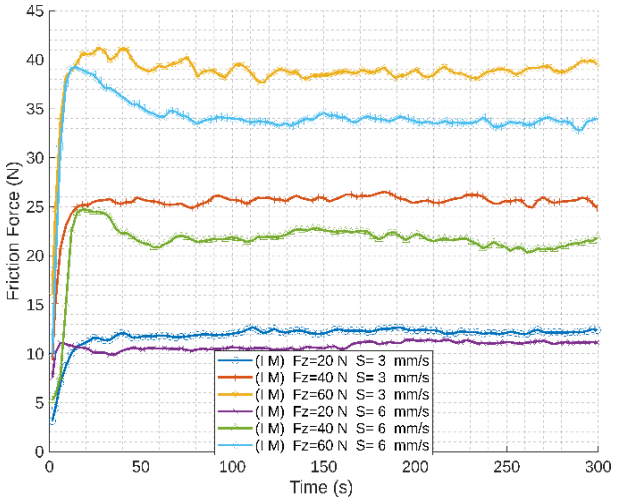

Fig. 21. Friction force for IM with different forces and speed.

Fig. 22 and Fig 23 show the effect of using lubrication in the wear test. It is clear from these graphs that the IL and IM cases in Wet cases have lower values than the dry cases as expected. It is also noticeable that in Wet cases the friction force is more stable, and the higher z force is more stable than the lower force. The gap difference between the levels of friction force is proportional to the value of the z force.

The difference between the friction force at 20N and 40N is higher than the difference between the friction force between 40N and 60N cases.

For IM dry cases, there is a jump at the beginning of the test, which is not the case for IL cases, nor is it the case for both IL and IM Wet cases.

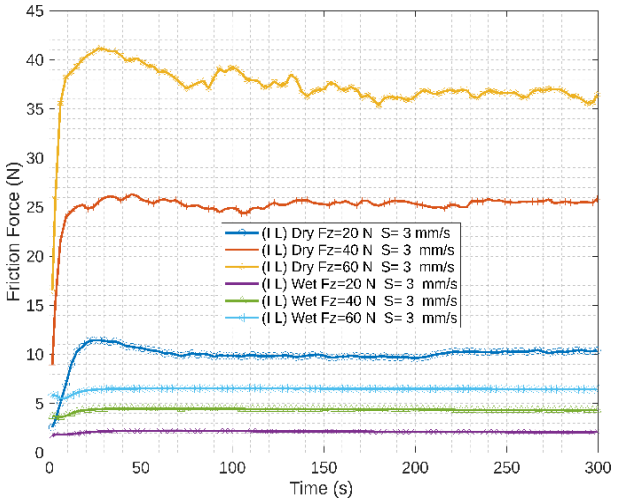

Fig. 22. Friction force for Wet IM and IL with different forces fixed speed.

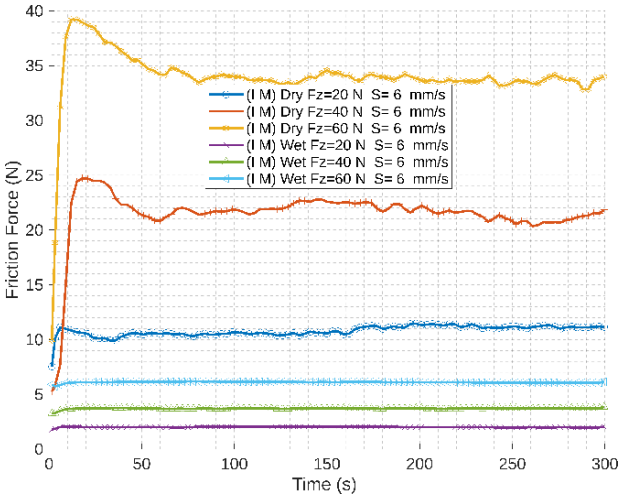

Fig 23. Friction force for dry and Wet IM with different forces and fixed speed.

3.5 Hardness

A micro-hardness test was done in different locations: in the re-melting area (the inter-layer area or overlapping area) and the middle of two different layers. Fig. 24 shows the location of the test numbered, and the results are shown in Table 4.

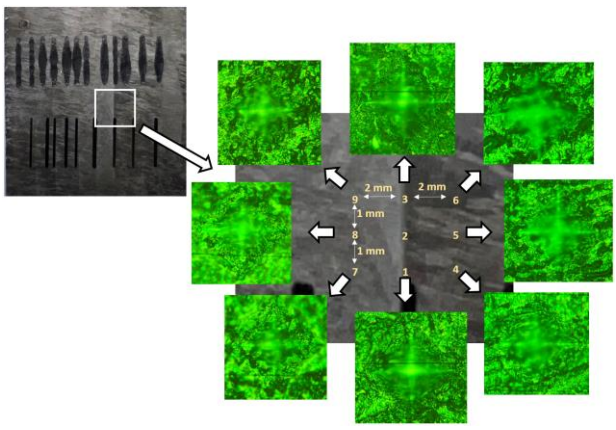

Fig. 24. Hardness measurement location around the IM and IL.

Table 4. Hardness results.

Location	HV	Average	Standard deviation
1	197.9	200.9	2.59
2	202.4		
3	202.4		
4	206.0	202.1	5.63
5	204.8		
6	195.7		
7	221.5	228.5	10.99
8	241.2		
9	222.9		

As reference hardness values, cast 316L had ~168 HV [46], SLM-ed ~225 HV [31], and CSAM-ed ~350 HV [32,46]. While all cases in WAAM have a higher level of hardness than the cast level. There are three groups, tests (1,2,3) are in the re-melting area which has an average of 200 HV, (4,5,6) are in the new layer which has an average of 202 HV, and (7,8,9) are in the previous layer which has an average of 228 HV. The results show that the previous layer has a hardness 14% higher than the re-melting and the new layer, which have the same level. For the first and second groups, the level of HV has increased by 20% while the previous layer that was affected by the heat but not melted has increased in HV by 35%. The results were the same for different materials, steel 347 printed by WAAM as well [47]. Generally a statement can be drawn that the IL in the re-melted areas has a lower hardness level due to its different thermal cycles. The microstructure of these areas has been studied; and the results show that the inter layer areas have columnar dendrites microstructure while the interlayer has a variation in the grain size [48,49].

4. CONCLUSIONS

This research investigates the wear behavior of a 316L austenitic stainless steel plate; which was printed by WAAM. A sample was machined and polished from the middle region of the plate. The wear tests were carried out in two regions, the IM and the IL, which are re-melted. The wear test is ball-on-flat, with different forces of 20, 40, and 60N, and different speeds of 3 and 6 mm/s using Wet and dry tests.

The results demonstrate that:

1. The coefficient of friction is 4% higher in IM than in IL. Doubling the speed increases the COF by 10-20%. The Wet cases have in general 1 to 6 to dry test in both IL and IM. The change of forces from 20, 40 to 60 has little effect on COF.
2. The average slope of COF is positive in IM areas and negative in IL areas, which leads to an increase in COF for IM and a decrease in COF for IL over time. However, using lubrication changes the average slope of COF in the IM trend to positive.

3. The volume and mass loss has the same observation. The Wet IL cases show an increase in both by 1%, which is different from IM.
4. The wear rate is a higher rate for Wet IL cases than IM cases by 1.5-3.5% depending on the force. As the force increases, the wear rate in both IL and IM cases becomes closer.
5. Friction force results show that IM cases have larger values in general than IL cases.
6. For hardness results, compared to the hardness of casted material, WAAM has increased the hardness. There are different levels of hardness according to the re-melted area IL which has lower hardness than the heated area IM.

In general, the re-melted area IL has a slight difference in the wear behavior than other areas in WAAM printed products. Also, IL has a lower hardness, COF, friction force, and COF slope. Which can be linked to its thermal cycles. As stated the interlayer areas have melted twice during printing time; which changes their microstructure; and that is the main aim for future research.

Acknowledgments

The author gratefully acknowledges Qassim University, represented by the Deanship of Scientific Research, on the financial support for this research under the number (20022-enuc-2021-1-2-w) during the academic year 1445 AH/2023 AD".

REFERENCES

[1] S. Chowdhury *et al.*, "Laser powder bed fusion: a state-of-the-art review of the technology, materials, properties & defects, and numerical modelling," *J. Mater. Res. Technol.*, vol. 20, pp. 2109–2172, Sep. 2022, doi: 10.1016/j.jmrt.2022.07.121.

[2] G. Gong *et al.*, "Research status of laser additive manufacturing for metal: a review," *J. Mater. Res. Technol.*, vol. 15, pp. 855–884, Nov. 2021, doi: 10.1016/j.jmrt.2021.08.050.

[3] R. Vaz, A. Garfias, V. Albaladejo, J. Sanchez, and I. Cano, "A Review of Advances in Cold Spray Additive Manufacturing," *Coatings*, vol. 13, no. 2, p. 267, Jan. 2023, doi: 10.3390/coatings13020267.

[4] N. Kumar *et al.,* "Wire Arc Additive Manufacturing – A revolutionary method in additive manufacturing," *Materials Chemistry and Physics*, vol. 285, p. 126144, Apr. 2022, doi: 10.1016/j.matchemphys.2022.126144.

[5] A. Alrumayh, "Residual Stresses Analysis of 3D Printed Plate By using Wire Arc Additive Manufacturing -WAAM-," Ph.D. dissertation, Lehigh University, Bethlehem, PA, USA, 2018.

[6] C. Sommitsch, N. Enzinger, P. Mayr, "Simulation of residual stresses during the wire arc additive manufacturing (WAAM) process," Mathematical Modelling of Weld Phenomena 13, Verlag der Technischen Universität Graz, Sep. 2023, pp. 283–303.

[7] A. Alrumayh, "Simulation of Crack Propagation for Additive Manufactured Components," Ph.D. dissertation, Lehigh University, Bethlehem, PA, USA, 2021.

[8] T. A. Rodrigues, *et al.,* "Wire and arc additive manufacturing of 316L stainless steel/Inconel 625 functionally graded material: development and characterization," *Journal of Materials Research and Technology,* vol. 21, pp. 237–251, Sep. 2022, doi: 10.1016/j.jmrt.2022.08.169.

[9] H. Ding, *et al.,* "Microstructure, mechanical properties and machinability of 316L stainless steel fabricated by direct energy deposition," *International Journal of Mechanical Sciences,* vol. 243, p. 108046, Dec. 2022, doi: 10.1016/j.ijmecsci.2022.108046.

[10] *Standard Test Method for Linearly Reciprocating Ball-on-Flat Sliding Wear*, ASTM G133, 2023.

[11] S. Nie, F. Lou, H. Ji, and F. Yin, "Tribological Performance of CF-PEEK Sliding against 17-4PH Stainless Steel with Various Cermet Coatings for Water Hydraulic Piston Pump Application," *Coatings*, vol. 9, no. 7, p. 436, Jul. 2019, doi: 10.3390/coatings9070436.

[12] C. Li, X. Deng, L. Huang, Y. Jia, and Z. Wang, "Effect of temperature on microstructure, properties and sliding wear behavior of low alloy wear-resistant martensitic steel," *Wear*, vol. 442–443, p. 203125, Nov. 2019, doi: 10.1016/j.wear.2019.203125.

[13] T. S. N. Sankara Narayanan, J. Kim, and H. W. Park, "High performance corrosion and wear resistant Ti-6Al-4V alloy by the hybrid treatment method," *Appl. Surf. Sci.*, vol. 504, p. 144388, Feb. 2020, doi: 10.1016/j.apsusc.2019.144388.

[14] J. Lu, *et al.*, "Effect of temperature on friction and galling behavior of 7075 aluminum alloy sheet based on ball-on-plate sliding test," *Tribology International,* vol. 140, p. 105872, Jul. 2019, doi: 10.1016/j.triboint.2019.105872.

[15] K. Nar, *et al.,* "Evaluating the effect of solid lubricant inclusion on the friction and wear properties of Laser Sintered Polyamide-12 components," *Wear*, vol. 522, p. 204873, Mar. 2023, doi: 10.1016/j.wear.2023.204873.

[16] A. K. Gain, *et al.,* "Wear mechanism, subsurface structure and nanomechanical properties of additive manufactured Inconel nickel (IN718) alloy," *Wear*, vol. 523, p. 204863, Mar. 2023, doi: 10.1016/j.wear.2023.204863.

[17] Z. Xu, *et al.,* "Tribological behaviors and microstructure evolution of Inconel 718 superalloy at mid-high temperature," *Journal of Materials Research and Technology,* vol. 14, pp. 2174–2184, Jul. 2021, doi: 10.1016/j.jmrt.2021.07.102.

[18] M. Tripathy, *et al.,* "Elevated temperature fretting wear study of additively manufactured inconel 625 superalloy," *Additive Manufacturing,* vol. 67, p. 103492, Mar. 2023, doi: 10.1016/j.addma.2023.103492.

[19] K. Zhang, *et al.,* "Microstructure and properties of composite coatings by laser cladding Inconel 625 and reinforced WC particles on non-magnetic steel," *Optics & Laser Technology,* vol. 163, p. 109321, Mar. 2023, doi: 10.1016/j.optlastec.2023.109321.

[20] J. Ge, *et al.,* "Investigation on H13 buildups produced with wire arc additive manufacturing: Deposition strategies-induced microstructural evolution and mechanical performances," *Journal of Alloys and Compounds,* vol. 860, p. 157893, Nov. 2020, doi: 10.1016/j.jallcom.2020.157893.

[21] S. Kumar, "Process chain development for additive manufacturing of cemented carbide," *Journal of Manufacturing Processes,* vol. 34, pp. 121–130, Jun. 2018, doi: 10.1016/j.jmapro.2018.05.036.

[22] X. Guo, I. Baker, F. E. Kennedy, and M. Song, "A comparison of the dry sliding wear behavior of NiCoCr medium entropy alloy with 316 stainless steel," *Materials Characterization*, vol. 160, p. 110132, Jan. 2020, doi: 10.1016/j.matchar.2020.110132.

[23] M. Krbata, M. Eckert, J. Majerik, and I. Barenyi, "Wear Behaviour of High Strength Tool Steel 90MnCrV8 in Contact with Si3N4," *Metals*, vol. 10, no. 6, p. 756, Jun. 2020, doi: 10.3390/met10060756.

[24] S. Cui *et al.*, "Tribological behavior comparisons of high chromium stainless and mild steels against high-speed steel and ceramics at high temperatures," *Friction*, vol. 10, no. 3, pp. 436–453, Jun. 2021, doi: 10.1007/s40544-021-0509-1.

[25] F. Lou, Z. Ma, S. Nie, H. Ji, and F. Yin, "A bidirectional wear model based on Inverse Gaussian (IG) process for PEEK against AISI630 stainless steel in seawater hydraulic components," *Tribology International*, vol. 175, p. 107815, Jul. 2022, doi: 10.1016/j.triboint.2022.107815.

[26] S. Yan *et al.*, "Carbon fiber cannot always reduce the wear of PEEK for orthopedic implants under DPPC lubrication," *Friction*, vol. 11, no. 3, pp. 395–409, Jun. 2022, doi: 10.1007/s40544-022-0604-y.

[27] S. Alkan and M. S. Gök, "Effect of sliding wear and electrochemical potential on tribocorrosion behaviour of AISI 316 stainless steel in seawater," *Engineering Science and Technology an International Journal*, vol. 24, no. 2, pp. 524–532, Aug. 2020, doi: 10.1016/j.jestch.2020.07.004.

[28] L. Wang *et al.*, "Sliding wear behavior and electrochemical properties of binder jet additively manufactured 316SS /bronze composites in marine environment," *Tribology International,* vol. 156, p. 106810, Dec. 2020, doi: 10.1016/j.triboint.2020.106810.

[29] S. H. Duntu, I. Ahmad, M. Islam, and S. Boakye-Yiadom, "Effect of graphene and zirconia on microstructure and tribological behaviour of alumina matrix nanocomposites," *Wear*, vol. 438–439, p. 203067, Sep. 2019, doi: 10.1016/j.wear.2019.203067.

[30] S. S. Cui *et al.*, "Detailed assessments of tribological properties of binder jetting printed stainless steel and tungsten carbide infiltrated with bronze," *Wear*, vol. 477, p. 203788, Mar. 2021, doi: 10.1016/j.wear.2021.203788.

[31] F. Bartolomeu *et al.,* "316L stainless steel mechanical and tribological behavior—A comparison between selective laser melting, hot pressing and conventional casting," *Additive Manufacturing*, vol. 16, pp. 81–89, May 2017, doi: 10.1016/j.addma.2017.05.007.

[32] R. F. Vaz, A. Silvello, J. Sanchez, V. Albaladejo, and I. G. Cano, "The Influence of the Powder Characteristics on 316L Stainless Steel Coatings Sprayed by Cold Gas Spray," *Coatings*, vol. 11, no. 2, p. 168, Jan. 2021, doi: 10.3390/coatings11020168.

[33] H. Li, M. Ramezani, M. Li, C. Ma, and J. Wang, "Effect of process parameters on tribological performance of 316L stainless steel parts fabricated by selective laser melting," Manufacturing Letters, vol. 16, pp. 36–39, Apr. 2018, doi: 10.1016/j.mfglet.2018.04.003.

[34] N. L. Parthasarathi, U. Borah, and S. K. Albert, "Effect of temperature on sliding wear of AISI 316 L(N) stainless steel – Analysis of measured wear and surface roughness of wear tracks," *Materials & Design (1980-2015),* vol. 51, pp. 676–682, May 2013, doi: 10.1016/j.matdes.2013.04.050.

[35] S. Alvi, K. Saeidi, and F. Akhtar, "High temperature tribology and wear of selective laser melted (SLM) 316L stainless steel," *Wear*, vol. 448–449, p. 203228, Feb. 2020, doi: 10.1016/j.wear.2020.203228.

[36] Y. Huang *et al.,* "Microstructure and wear properties of selective laser melting 316L," *Materials Chemistry and Physics*, vol. 254, p. 123487, Jul. 2020, doi: 10.1016/j.matchemphys.2020.123487.

[37] L. D. Tadepalli *et al.,* "Microstructure analysis and wear characterization of AISI 316 austenitic stainless steel by cyaniding process," *Materials Today Proceedings*, vol. 44, pp. 1455–1458, Jan. 2021, doi: 10.1016/j.matpr.2020.11.633.

[38] M. Peruzzo, F. L. Serafini, M. F. C. Ordoñez, R. M. Souza, and M. C. M. Farias, "Reciprocating sliding wear of the sintered 316L stainless steel with boron additions," *Wear*, vol. 422–423, pp. 108–118, Jan. 2019, doi: 10.1016/j.wear.2019.01.027.

[39] C. V. Haden, G. Zeng, F. M. Carter, C. Ruhl, B. A. Krick, and D. G. Harlow, "Wire and arc additive manufactured steel: Tensile and wear properties," A*dditive Manufacturing*, vol. 16, pp. 115–123, May 2017, doi: 10.1016/j.addma.2017.05.010.

[40] C. Sánchez de Rojas Candela, A. Riquelme, P. Rodrigo, B. Torres, and J. Rams, "Wear behavior of additively manufactured 316L/SiCp composites with up to 60 wt% SiCp," *Ceram. Int.*, vol. 48, no. 22, pp. 33736–33750, Nov. 2022, doi: 10.1016/j.ceramint.2022.07.319.

[41] Y. Yang, *et al.*, "Wear anisotropy of selective laser melted 316L stainless steel," *Wear*, vol. 428–429, pp. 376–386, Apr. 2019, doi: 10.1016/j.wear.2019.04.001.

[42] H. Li, *et al.*, "Tribological performance of selective laser melted 316L stainless steel," *Tribology International,* vol. 128, pp. 121–129, Jul. 2018, doi: 10.1016/j.triboint.2018.07.021.

[43] S. M. Yusuf, D. Lim, Y. Chen, S. Yang, and N. Gao, "Tribological behaviour of 316L stainless steel additively manufactured by laser powder bed fusion and processed via high-pressure torsion," *Journal of Materials Processing Technology*, vol. 290, p. 116985, Nov. 2020, doi: 10.1016/j.jmatprotec.2020.116985.

[44] G. Özer, A. Kisasoz, "The role of heat treatments on wear behaviour of 316L stainless steel produced by additive manufacturing," *Materials Letters,* vol. 327, p. 133014, Aug. 2022, doi: 10.1016/j.matlet.2022.133014.

[45] P. L. Menezes, M. Nosonovsky, S. V. Kailas, and M. R. Lovell, "Friction and Wear," *Springer*, 2013, pp. 43–91. doi: 10.1007/978-1-4614-1945-7_2.

[46] R. M., L. M., K. H., and S. V. P., "Mechanical and tribological properties of SS316L with comparison of SLM and casting methods," *Mater. Today Proc.*, Apr. 2023, doi: 10.1016/j.matpr.2023.03.333.

[47] R. Duraisamy, *et al.*, "Tribological performance of wire arc additive manufactured 347 austenitic stainless steel under unlubricated conditions at elevated temperatures," *Journal of Manufacturing Processes,* vol. 56, pp. 306–321, May 2020, doi: 10.1016/j.jmapro.2020.04.073.

[48] W. Jin, C. Zhang, S. Jin, Y. Tian, D. Wellmann, and W. Liu, "Wire Arc Additive Manufacturing of Stainless Steels: A Review," *Appl. Sci.*, vol. 10, no. 5, p. 1563, Feb. 2020, doi: 10.3390/app10051563.

[49] C. Sasikumar and R. Oyyaravelu, "Mechanical properties and microstructure of SS 316 L created by WAAM based on GMAW," *Mater. Today Commun.*, vol. 38, p. 107807, Mar. 2024, doi: 10.1016/j.mtcomm.2023.107807.